INTERNATIONAL JOURNAL FOR NUMERICAL METHODS IN ENGINEERING
Int. J. Numer. Meth. Engng 2004; **60**:1139–1159 (DOI: 10.1002/nme.1000)

Quality improvements in extruded meshes using topologically adaptive generalized elements

Satish Chalasani*, † and David Thompson

Computational Simulation and Design Center at the ERC, Mississippi State University, Mississippi State, MS 39762, U.S.A.

SUMMARY

This paper describes a method to extrude near-body volume meshes that exploits topologically adaptive generalized elements to improve local mesh quality. Specifically, an advancing layer algorithm for extruding volume meshes from surface meshes of arbitrary topology, appropriate for viscous fluid flows, is discussed. First, a two-layer reference mesh is generated from the layer initial surface mesh by extruding along the local surface normals. The reference mesh is then smoothed using a Poisson equation. Local quality improvement operations such as edge collapse, face refinement, and local reconnection are performed in each layer to drive the mesh toward isotropy and improve the transition from the extruded mesh to a void-filling tetrahedral mesh. A few example meshes along with quality plots are presented to demonstrate the efficacy of this approach. Copyright © 2004 John Wiley & Sons, Ltd.

KEY WORDS: extrusion; hybrid mesh; Poisson smoothing; generalized elements; edge collapse; face refinement

1. INTRODUCTION

Mesh generation remains a major bottleneck in the routine simulation of viscous fluid flows. Generation of a multi-block structured grid for a complex configuration is a labour-intensive process. In comparison, an unstructured tetrahedral mesh can be generated regardless of the complexity of the geometry. The main disadvantages associated with tetrahedral meshes are the memory required (which is significantly larger than the memory required for a hexahedral mesh of the same point density) and questions regarding the accuracy of computations on highly anisotropic tetrahedra [1]. Hybrid meshes have the advantages of both structured and unstructured meshes. In a hybrid mesh, a highly stretched, near-body mesh is extruded from the surface to capture large gradients in the field variables. The extruded mesh is typically generated using an advancing layer scheme [2–4]. The remainder of the domain is filled with

*Correspondence to: Satish Chalasani, Computational Simulation and Design Center, P.O. Box 9627, Mississippi State, MS 39762-9627, U.S.A.
†E-mail: satish@erc.msstate.edu

Received 14 June 2002
Revised 15 October 2002
Accepted 25 August 2003

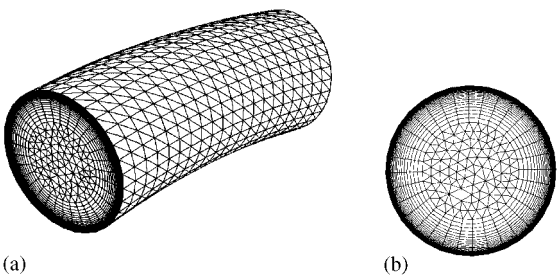

Figure 1. Example of a hybrid mesh—simple curved pipe: (a) volume mesh; and (b) mesh at the inlet of the pipe.

a nearly isotropic tetrahedral mesh. If the initial surface mesh has quadrilaterals, some type of transitional element is needed between the extruded mesh and the tetrahedral mesh. A simple example of a hybrid mesh is shown in Figure 1. In this example, the initial surface mesh consists of triangles resulting in triangular prisms in the near-body mesh. The composite mesh has a smooth variation near the interface of the near-body and tetrahedral meshes. Typically, in a hybrid mesh, all elements are of standard shapes: triangular prisms and tetrahedra or hexahedra, pyramids, and tetrahedra.

Unfortunately, volume meshes generated using advancing layer methods may have poor quality elements near convex and concave regions of the geometry. These elements may adversely affect the transition between the near body mesh and void filling tetrahedral mesh. To address this shortcoming, several researchers have considered the possibility of using other element types to improve local mesh quality [5–7]. The resulting meshes, which may contain arbitrary polyhedra with no restrictions placed on the number of edges a face can have or the number of faces a element can have, have been dubbed generalized meshes [8].

Thompson and Soni [5] employed face termination and face refinement to improve mesh quality near convex and concave regions of the geometry. Their strategy resulted in the production of general elements with 'hanging nodes' and was limited to structured quadrilateral surface meshes.

Leatham *et al.* [6] employed edge collapse and edge refinement to achieve the same objectives. Their approach utilized non-face matching, i.e. a face of one element need not be coincident with a face in the adjacent element. The mismatch is caused by the application of face refinement to the initial surface before the extrusion step and imposes additional requirements on the flow solver. This method can be used for any initial surface mesh topology.

Cary and Michal [7] introduced the concept of a 'generalized prism' to improve the quality of the mesh. An element denoted as a 'filler cell,' obtained by collapsing one of the triangular faces of a prism to a line segment, is employed to improve quality near concave/convex regions. In order to control the resolution of the mesh near convex regions, degenerate triangles (lines/points) are added on the initial triangulated surface mesh so that, when extruded from these entities, the resultant faces will have finite areas and the 'filler cells' formed out of these degenerate faces will have finite volumes. Due to the addition of degenerate faces on the initial surface, new extrusion directions must be computed.

For a hybrid mesh with basic element types, Marcum [9] developed a technique to provide a smooth transition between the near-body mesh and the void-filling tetrahedral mesh by

terminating the extruded mesh locally when the algorithm tries to insert a new point close to an existing point or if the spacing is comparable to the initial surface mesh spacing. However, this approach may result in a premature transition to tetrahedral elements. Additionally, this approach was developed in the context of an advancing front algorithm and is not appropriate for an advancing layer algorithm.

It should be noted that there are performance penalties associated with CFD solvers designed to use meshes containing general elements when compared to solvers developed for specific element types. However, the HYB3D code [8], the COBALT code [10], and the CHEM code [11] have demonstrated the efficacy of generalized mesh technology.

In this paper, we present a novel technique to extrude volume meshes that exploits topologically adaptive generalized elements to improve local mesh quality. There are several differences in the approach described here and those described in the above-mentioned references. A Poisson smoothing operation, which is described in detail in Reference [12], is applied to the actual point positions rather than the extrusion normals. Further, the quality improvement operations consist of edge collapse and face refinement based on geometric properties of faces in the marching direction followed by face splitting and reconnection based on geometric properties of faces in the extruded surface. Face matching between elements is enforced throughout the procedure and no degenerate faces are added to the mesh.

The approach described here, as well as the others described above, can be contrasted with the approach described in Reference [4], which adjusts the mesh locally to avoid collisions between advancing layers. The local geometric criteria employed to trigger the topological operations are inadequate to detect these 'non-local collisions.' Therefore, another strategy must be employed. Our strategy for dealing with these collisions, which is based on a combination of extrusion step-size reduction and face refinement, will be described in a future paper.

2. OUTLINE OF THE EXTRUSION ALGORITHM

The following advancing layer algorithm for generating near-body volume meshes is based on a parabolic mesh generation algorithm [13] modified to extrude volume meshes from surface meshes of arbitrary topology. Elements in each layer of the mesh are made up of faces belonging to the initial surface for the layer, the extruded surface, and the marching faces. Marching faces are those which connect edges in the initial surface mesh to the corresponding edges on the extruded surface mesh. Since the elements are extruded, these faces will be quadrilaterals regardless of the surface mesh topology. Before applying quality improvements, faces in the extruded surface will have the same topology as the initial surface mesh for the layer. The extruded face and marching face topologies may change after applying the quality improvements. Depending on the topology of the domain being meshed, i.e. if the surface being extruded from is not closed, the extrusion may have 'side' boundaries. Nodes and edges located on these side boundaries are called boundary nodes and edges, respectively.

The following three-step process is used to generate each layer of the mesh. Please refer to Figure 2.

(i) *Generate the reference mesh*—generate two layers of a reference mesh, k and $k+1$, by extruding from an initial surface mesh, points 1, 2, and 3, in the direction of the local surface normals. A simple way to compute a normal direction at a given node is to

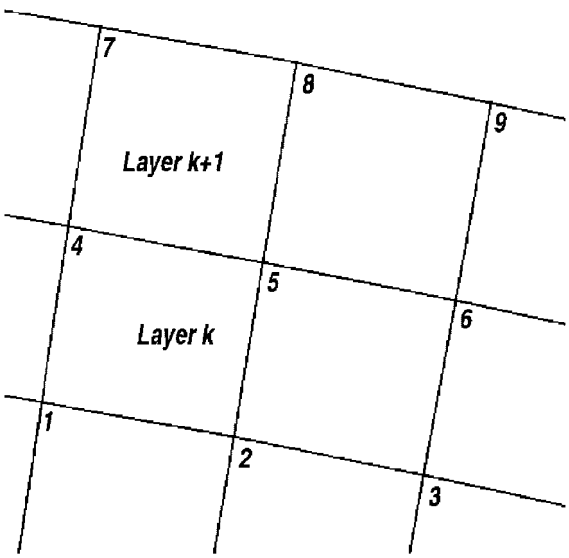

Figure 2. Reference mesh.

take a weighted average of face normals sharing the node under consideration. However, after extrusion, the resulting point location may violate the visibility condition [4] if the surface has sharp discontinuities, for example, at the intersection of a wing trailing edge and a fuselage. Kallinderis [4] describes a method to find a normal direction that satisfies the visibility condition.

(ii) *Smooth the reference mesh*—smooth the interface between the first and second layers of the reference mesh, points 4, 5, and 6, using a Poisson equation [12]. Update the outer surface of the second layer of the reference mesh, points 7, 8, and 9, after every iteration. The Poisson equation is obtained by modifying the method described in Reference [14] for smoothing surface meshes of arbitrary topology. Control functions are used to maintain the characteristics of the initial surface. Note that the actual point positions are adjusted using this smoothing. Boundary nodes are smoothed according to the boundary conditions specified. Generally, three kinds of boundary conditions are encountered:

   (a) *Constrained*—the boundary normals are constrained to lie within a specified plane.
   (b) *Floating*—the boundary is allowed to float based on local surface normal.
   (c) *Fixed*—the normal direction is specified.

(iii) *Perform quality improvements*—after smoothing, perform local mesh quality improvements on the extruded surface of the first layer, points 4, 5, and 6, and discard the outer surface of the second layer, points 7, 8, and 9. Then, update the face and element connectivities to reflect the changes due to quality improvements. The outer surface of the first layer of the mesh, points 4, 5, and 6, is used as the initial surface for the next layer.

The above three steps are repeated until the desired number of layers is extruded. More details regarding the extrusion process can be found in Reference [12]. We now focus on the topological operations used to improve mesh quality after smoothing. It should be noted that these operations may be performed independently of the method employed to extrude the mesh.

3. MESH QUALITY IMPROVEMENT

3.1. Element quality

The first point that must be addressed is the general issue of element quality. This topic has been studied extensively and is well understood for simplex elements such as triangles and tetrahedra [15]. Wa and Chen [16] attempted to quantify quality for hexahedral and prismatic elements using a combination of face properties to define a quality metric. Inherent to this approach is the assumption that a volume element is of good quality if its faces are of good quality. Following a somewhat different approach, Owen *et al.* [17] examined the quality of a pyramidal element by decomposing it into tetrahedral elements and then applying the tetrahedral element quality metric to the resultant elements. Obviously, this approach depends on the procedure followed to decompose the pyramid.

The approach taken here is modelled after the face-based decomposition employed in Reference [16]. This approach is particularly appropriate for general elements since the decomposition of an arbitrary polyhedron into tetrahedral elements may not always be a straightforward process. A high quality triangular face is taken to be one that is isotropic while a high quality quadrilateral face is one that is rectangular. It is not clear what configuration constitutes a quality *n-gon*.

In general, it is difficult to assess the quality of a general volume element since, for non-simplex elements, even notions of convexity must be abandoned. However, a nominal requirement is that the element centroid must be located in the interior of the element. The only time this condition is violated for an element that is not obviously 'defective' is for a highly anisotropic extruded element with twisted quadrilateral faces.

3.2. Mesh quality improvement strategy

In essence, the face-based notion of mesh quality reduces the determination of element quality to the determination of the quality of each of the faces that constitute the element. Figure 3(a) shows an example of poor quality elements near a concave region when extruded from the

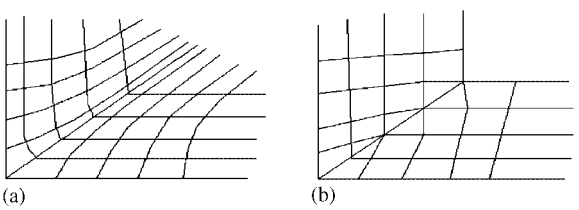

Figure 3. Edge collapse improves mesh quality near concave regions: (a) without edge collapse; and (b) with edge collapse.

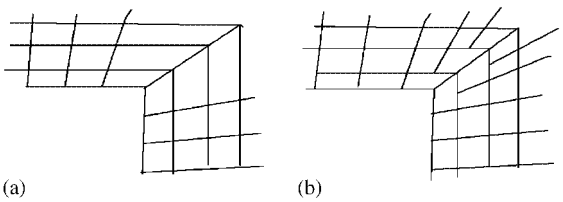

Figure 4. Face refinement improves mesh quality near convex regions: (a) without face refinement; and (b) with face refinement.

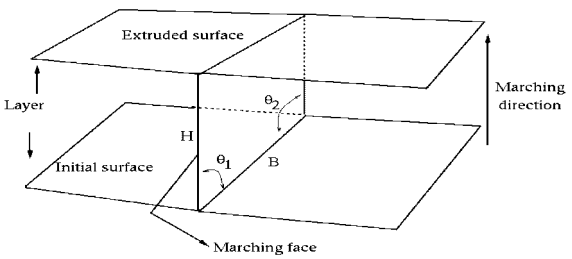

Figure 5. Extruded mesh nomenclature.

initial surface mesh. As this mesh is extruded, poor aspect ratio elements develop that will produce 'slivers' in the tetrahedral mesh. Additionally, the transition between the extruded mesh and the tetrahedral mesh will be poor. The solution to this problem proposed here and elsewhere [5–7] is to employ a change in the local element topology. Edge collapse, as shown in Figure 3(b), stops the generation of poor quality elements and provides the opportunity to extrude further into the domain. Figure 4(a) shows poor quality elements near convex regions of the geometry. Face refinement, as shown in Figure 4(b), improves the quality of the mesh by improving the aspect ratio of the elements. However, since these operations may lead to poor quality on the extruded surface of each layer, quality improvement operations should be performed on the extruded surface as well.

Notice that each of the operations discussed above is applied to the faces of a element, which is consistent with the notion of element quality proposed above, based on local geometric sensors. The quality improvement process starts with edge collapse followed by face refinement. For complex three-dimensional geometries, these geometric sensors may produce conflicting requirements at a few isolated locations causing faces/edges to be selected for both collapse and refinement. In these cases, edge collapse is given precedence to avoid mesh crossing in concave regions.

The specific operations employed to improve mesh quality are discussed in the following sections. The terms listed below are used in the discussion of the quality improvements:

(i) The *face aspect ratio* is defined as the ratio of the longest edge to the smallest edge in a face. This is defined for each face in the extruded surface and the initial surface of each layer as shown in Figure 5.

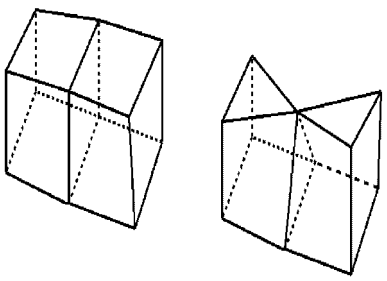

Figure 6. Edge collapse operation—before and after.

(ii) The *element aspect ratio* is defined as the ratio of the extruded face aspect ratio to the initial face aspect ratio.
(iii) The *marching face aspect ratio* is defined as the ratio of the edge length in the marching direction to the edge length on the initial surface. In Figure 5, the marching face aspect ratio is given by H/B. Marching faces are formed by connecting edges on the initial surface to corresponding edges on the extruded surface.
(iv) The *divergence angle* is defined for each edge and is defined as the maximum of angles (θ_1, θ_2) in Figure 5.
(v) The *nodal length scale* is defined as the average of length of the edges incident on a node. If N edges are on a node, the nodal length scale is given by

$$\frac{1}{N}\sum_{i=1}^{N} \text{edge length}_i$$

3.2.1. Edge collapse. Edge collapse is performed to improve the quality of the mesh near concave regions and to force the mesh to become more isotropic. Only edges in the extruded surface of the layer are considered for collapse. In general, edge collapse reduces the number of edges of an element in the extruded surface by one. Edge collapse for a triangular face produces a single edge. Edge collapse always results in a triangular marching face.

Figure 6 shows a schematic description of the edge collapse operation. As shown in Figure 7, there are three possible ways in which an edge can be collapsed: either end or the midpoint. The choice depends on the type of edge. The boundary nodes and edges, if they exist for a given mesh, lie in marching faces on the side boundaries of the mesh. There are four distinct types of edges:

(i) An edge that is not connected to a boundary node of the extruded surface mesh, i.e. a completely internal edge of the extruded surface mesh.
(ii) An edge where one node is a boundary node of the extruded surface mesh.
(iii) A boundary edge where both nodes have the same boundary condition type.
(iv) A boundary edge where the two nodes have different boundary conditions. For example, if the boundary condition for one node is 'constrained' and the boundary condition for the other is 'fixed,' the edge is collapsed to the node with the 'fixed' boundary condition. This case is normally only encountered at boundaries with sharp corners in the extruded surface mesh.

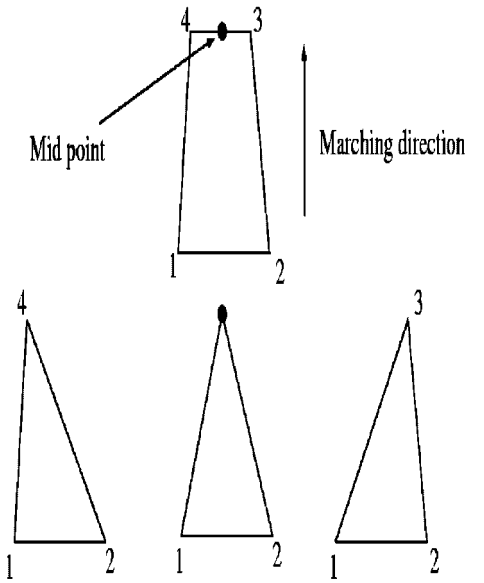

Figure 7. Edge collapse—left, midpoint, and right.

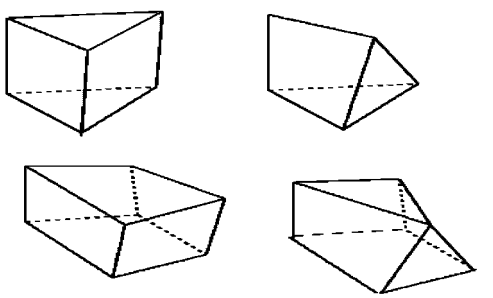

Figure 8. Resultant generalized element topologies when one edge is collapsed for a prism (top) and a hexahedron (bottom).

If the selected edge is of type (i) or (iii), midpoint subdivision is used as the other two options will result in a non-uniform change in nodal length scale which in turn results in skewed faces in the marching direction. If the selected edge of type (ii) or (iv), then one or the other node is chosen to maintain boundary integrity. The resulting element topology after edge collapse depends on the number of edges selected for collapse. If the face on the initial surface is a triangle or a quadrilateral and one of its edges is selected for collapse, the resultant generalized element is as shown in Figure 8. In the case of a quadrilateral, if two edges are selected then, the collapse operation results in a wedge.

The edges to be collapsed are selected according to the following criteria:

(i) The *element aspect ratio* is used to identify converging elements near non-convex regions that will produce slivers in the tetrahedral mesh. For each marching face, this ratio is calculated for the two elements sharing the face. If the marching face is a boundary face, then it will be a member of only a single element. If this ratio is greater than a specified threshold, then the edge is marked for collapse. Based on the authors' experience, a good range for this threshold is a 20–40 per cent increase.
(ii) The *marching face aspect ratio* is used to trigger edge collapse for marching faces. This ratio identifies faces that will produce slivers in the tetrahedral mesh. The threshold values are specified so that the resultant triangular marching face will be closer to isotropic. The ideal threshold value is 0.866 which is the length of the bisector of an equilateral triangle. Values in the range of 0.7 to 0.9 have been shown to produce acceptable results.

Each edge marked for collapse is assigned a priority according to the marching aspect ratio and are sorted according to this priority. The edge collapse process is initiated at the first edge in the list. To avoid performing an operation that results in an invalid mesh, all of the edges sharing either of the two nodes of the edge under consideration are marked as non-collapsible edges. Before performing the edge collapse operation, the volume of the element is checked to ensure that the mesh remains valid. After each operation the face/element connectivity is updated to reflect the changes.

3.2.2. Face refinement. Face refinement is performed to improve the mesh quality near convex regions and to force the mesh to become more isotropic. Selected edges of the extruded surface are bisected and the face connectivity in the extruded surface is updated according to the number of edges selected. For each refined face, its connectivity in the marching direction is updated from a quadrilateral to a generalized topology. The selected faces are refined and the element connectivity is updated.

Edges are marked for refinement based on the *divergence angle* which quantifies the degree of divergence of a mesh face. The divergence angle is calculated for each marching face in the layer. If the angle is greater than the threshold, the edge is marked for refinement. Based on the authors' experience, threshold values near 115° are appropriate. Figures 9 and 10 show the strategies employed here for refining a hexahedral element and a prismatic element, respectively. Both strategies are designed to produce only triangles and quadrilaterals in the extruded surface.

3.2.3. Extruded surface mesh improvement. The edge collapse and face refinement operations described above improve the quality along the marching direction. However, these operations do not take into account the quality of the mesh in the extruded surface which may become degraded. The following steps are applied locally to the extruded surface mesh to improve the mesh quality. These steps are designed in a such a way that the resultant extruded surface will have only triangles and quadrilaterals.

(i) A *skewed quadrilateral face* can be converted into two triangles of higher quality. This operation is called face splitting. If necessary, splitting of all quadrilateral faces can be used in the last extruded surface to make it compatible with tetrahedral meshing.
(ii) The *triangle with a 'needle' shape* shown in Figure 11(a), in addition to being of poor quality, will produce sliver elements in the tetrahedral mesh. These triangles can be

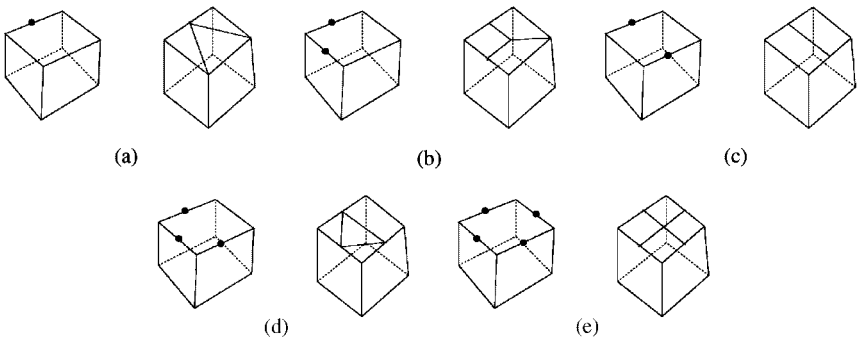

Figure 9. Refinement strategies for a hexahedral element according to the number of marked edges: (a) one edge marked; (b) two adjacent edges marked; (c) two non-adjacent edges marked; (d) three edges marked; and (e) four edges marked.

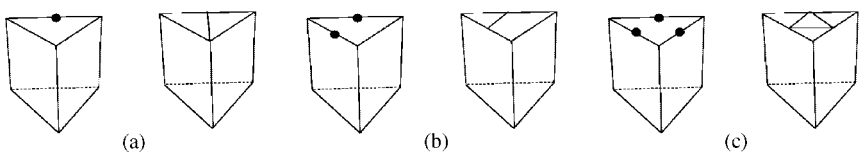

Figure 10. Refinement strategies for a prismatic element according the number of selected edges: (a) one edge marked; (b) two edges marked; and (c) three edges marked.

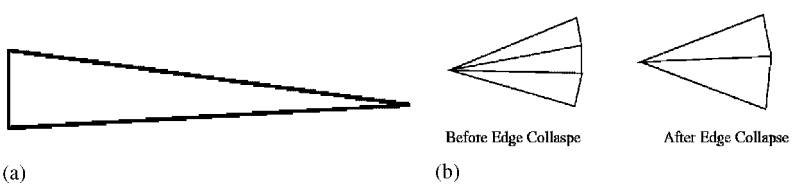

Figure 11. Quality improvement by edge collapse: (a) skewed triangle or 'needle'; and (b) edge collapse improves the mesh quality locally.

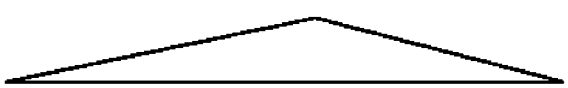

Figure 12. Skewed triangle with large obtuse angle.

eliminated by edge collapse. The shortest edge is identified and collapsed to its midpoint as shown in Figure 11(b). Triangles with large obtuse angles, shown in Figure 12, also result in slivers in the tetrahedral mesh. These faces can be eliminated by changing the local connectivity according to the type of face sharing its longest edge. There are three

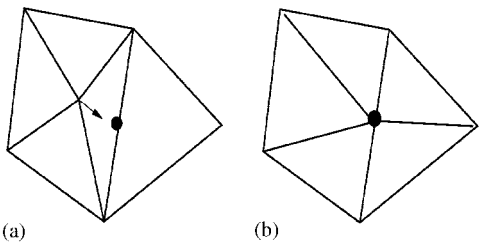

Figure 13. Quality improvement when the longest edge of the skewed face is shared by a better quality triangle: (a) before; and (b) after.

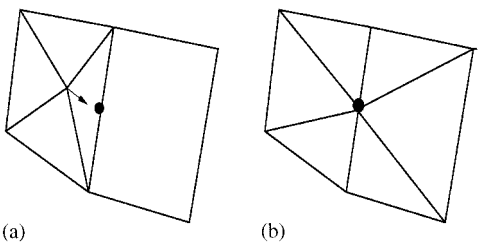

Figure 14. Quality improvement when the longest edge of the skewed face is shared by a better quality quadrilateral: (a) before; and (b) after.

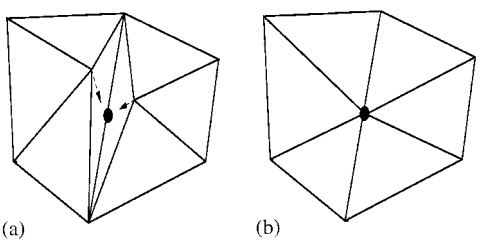

Figure 15. Quality improvement when the longest edge of the skewed face is shared by a skewed triangle: (a) before; and (b) after.

types generally encountered:

(a) In Figure 13(a), the face that shares the edge is a better quality triangle. To improve the quality of the mesh, a node which is not a part of the shared edge is snapped to the midpoint of the longest edge and the neighbouring face connectivity is updated by splitting the triangular face into two triangles as shown in Figure 13(b).
(b) In Figure 14(a), the face that shares the edge is a better quality quadrilateral. The face connectivity is modified by splitting it into three triangles as shown in Figure 14(b).
(c) In Figure 15(a), the face that shares the edge is also a triangular face with a large obtuse angle. Local mesh quality is improved by snapping the two nodes to the

midpoint of the longest edge as shown in Figure 15(b). Standard operations like edge swapping cannot be applied here because operations done on the surface also affect the faces in the marching direction. Smoothing cannot be applied because, in the process of smoothing the surface mesh, orthogonality may be lost along the marching direction.

Quality improvement operations in the extruded surface are designed to minimize the differences in local nodal length scales, before and after the operations in the extruded surface mesh.

3.3. Data structures

The data structure plays an important role in implementing any mesh generation algorithm. The software developed by the authors is written in C + + using vectors and lists available in the standard template library. The data structure is face based, similar to the radial edge data-structure. Each face has a pointer to elements that share it. Attributes like aspect ratio, normal, angle, and node information are stored for each face. A face can be a triangle, a quadrilateral, or a five-sided polygon. There is no restriction on the number of faces a element can have. The number of nodes can be different from its previous layer, but there will be face to face match between consecutive layers.

4. RESULTS

A few example meshes are now presented to demonstrate the approach described in the text. The volume mesh generated for each example is output in the face-based COBALT mesh format [18]. VTK [19] is used for visualizing the volume meshes. Plots of the face-based quality metrics for the outer layer of each mesh (which will be used as a starting point to generate the tetrahedral mesh) are included to demonstrate the effectiveness of the quality improvements. Plots of the extruded surface aspect ratio are included to illustrate the deviation from isotropy. Plots of the marching aspect ratio help to quantify the smoothness of the transition between the extruded mesh and tetrahedral mesh. Since plots of the extruded surface aspect ratio alone do not provide sufficient information about the skewness of the faces in the extruded surface mesh, plots of the minimum angles for quadrilaterals and triangles are also included. The meshes are intentionally coarse so that the behaviour of the mesh generation algorithm is more obvious.

The first example is a simple surface of revolution. The surface mesh has 1320 nodes with 1296 quadrilateral faces. Figures 16(a) and (b) show the cross-section and outer surface of the volume mesh. The mesh was extruded seven layers with floating boundary conditions and consisted of 9072 elements. Figure 16(c) shows the quality plots for the last layer. Due to clustering of the lines emanating from the concave regions, several faces on the extruded surface of the last layer have aspect ratios greater than 15 and a few faces in the marching direction have aspect ratios greater than 2.5. This is more prominently visible on the outer surface of the mesh as shown in Figure 16(b). The cross section and the outer surface of the volume mesh generated by extruding the same number of layers with quality improvements are shown in Figures 17(a) and (b), respectively. Face refinement is triggered near the sharp corners in the surface mesh which increases the number of elements. As the mesh is extruded further, edge collapse is triggered and eliminates a few faces in each layer. The net result is that the

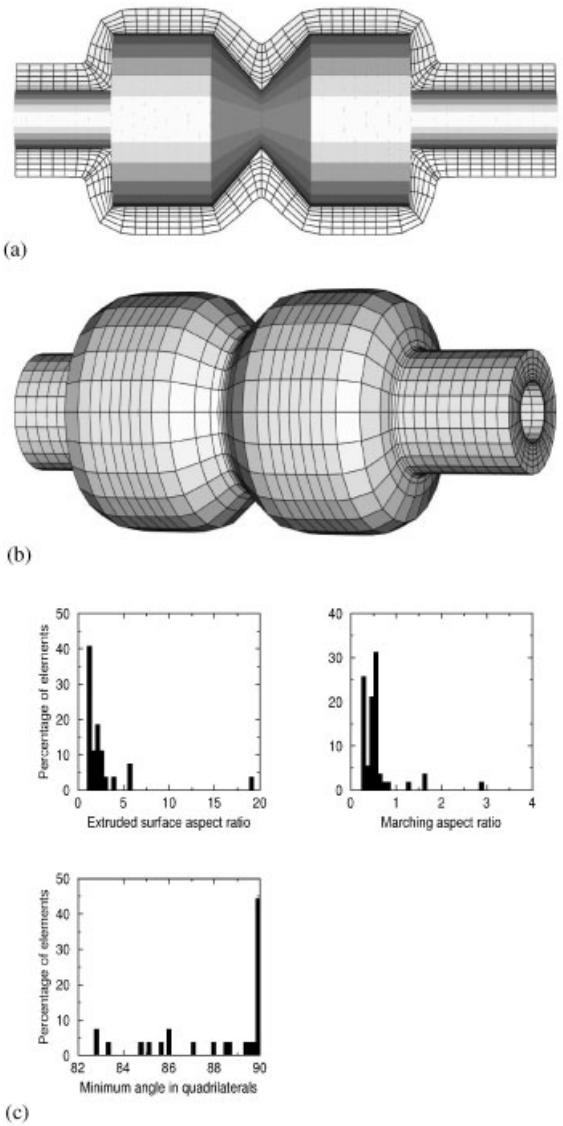

Figure 16. Volume mesh for surface of revolution generated by extruding seven layers without quality improvements: (a) cross section of the volume mesh; (b) outer surface mesh of the volume mesh; and (c) quality plots for the last layer of the volume mesh.

number of faces in the outer surface mesh decreases from 1296 in the initial surface mesh to 1152 while the number of elements increases from 9072 to 9336. This result is primarily due to the fact that the layer extrusion distance is increased in each layer so that more elements are located near the initial surface where the refinement occurs. Quality plots for the last layer

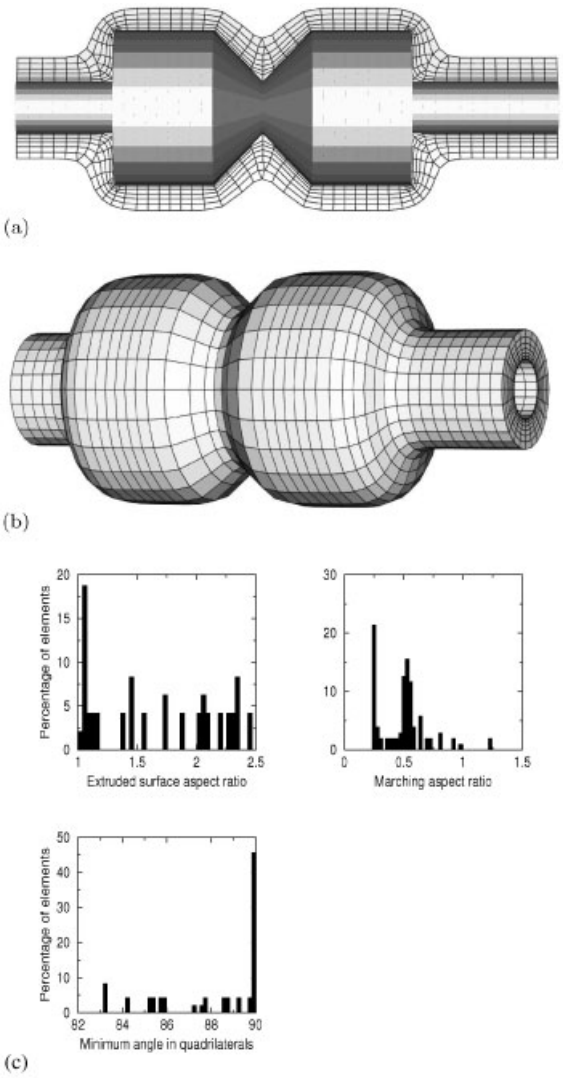

Figure 17. Volume mesh for surface of revolution generated by extruding seven layers without quality improvements: (a) cross section of the volume mesh; (b) outer surface mesh of the volume mesh; and (c) quality plots for the last layer of the volume mesh.

are shown in Figure 17(c). These plots indicate that the maximum extruded surface aspect ratio is less than 2.5 and the maximum marching aspect ratio is less than 1.5. The quality plots indicate improvement in mesh quality according to the face-based quality metrics. Additionally, the mesh can be extruded further without front collisions due to the quality improvements. The cross section and outer surface of the volume mesh obtained after extruding 15 layers are shown in Figures 18(a) and (b). These figures show a more uniform mesh on the outer surface.

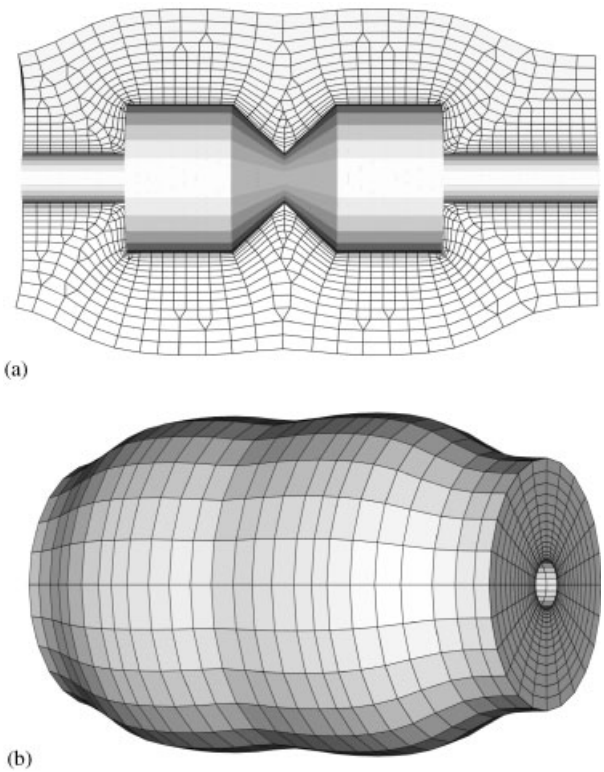

Figure 18. Volume mesh for surface of revolution generated by extruding 15 layers with quality improvements: (a) cross section of full extruded volume mesh; and (b) outer surface mesh of the volume mesh.

The cross section shows clearly how edge collapse and face refinement work as the mesh is extruded.

The second example is a notional 'x38-like' geometry. The initial surface mesh consists of 9694 quadrilateral faces, 100 triangular faces, and 9795 nodes. The resulting volume mesh consisting of 68558 elements is generated by extruding seven layers without quality improvements. The cross section and outer surface of the volume mesh are shown in Figure 19(a) and (b), respectively. The quality plots for the last layer shown in Figure 19(c) show extruded surface aspect ratios greater than 9 and marching aspect ratios greater than 10. The plots also indicate the outer surface mesh has a few quadrilateral faces with angles less than 40° and a few triangular faces with angles less than 10°. This is because the quadrilateral faces and triangular faces near concave regions become more skewed during the extrusion process. The cross section and outer surface of the 52945 element volume mesh generated by extruding the same number of layers with quality improvements are shown in Figures 20(a) and (b), respectively. In the outer surface, the number of faces is reduced from 9794 to 2871 and the number of nodes is reduced from 9795 to 1621 nodes. The quality plots for the last layer of the mesh generated are shown in Figure 20(c). The quality plots indicate the maximum extruded

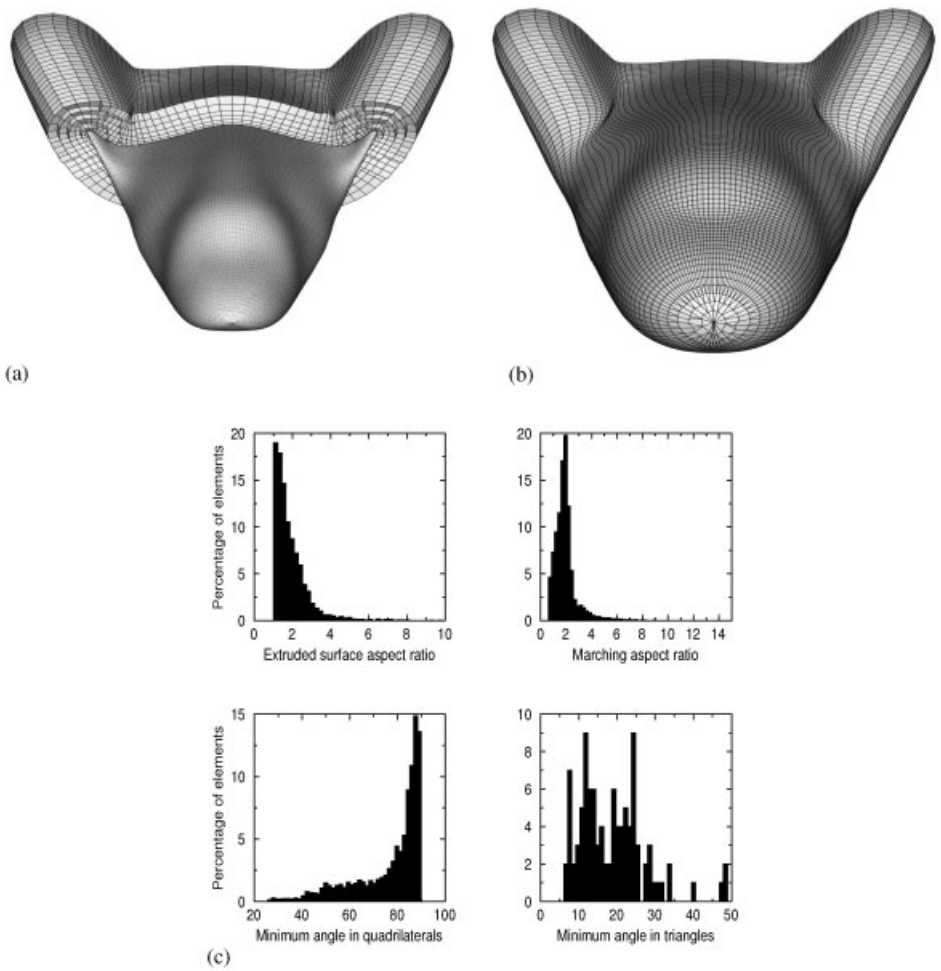

Figure 19. Notional x38 volume mesh generated by extruding seven layers without quality improvements: (a) cross section of the volume mesh; (b) outer surface mesh of the volume mesh; and (c) quality plots of the last layer of the volume mesh.

surface aspect ratio is less than 3.1 and the maximum marching aspect ratio is less than 2.2. The minimum angles in quadrilateral faces and triangular faces are also improved. The cross section and outer surface of a volume mesh generated by extruding 15 layers are shown in Figures 21(a) and (b), respectively. Figure 21(c) shows a rear view of the fully extruded mesh. These images clearly illustrate how the quality improvements force the mesh elements toward isotropy.

The third example is a tactical aircraft geometry (courtesy of T. Michal, Boeing). The relatively coarse surface mesh with sharp convex and concave regions consists of 6779 nodes and 13554 triangles. This example shows that the quality improvement operations are effective independent of the initial surface mesh topology and geometric complexity. Figure 22 shows

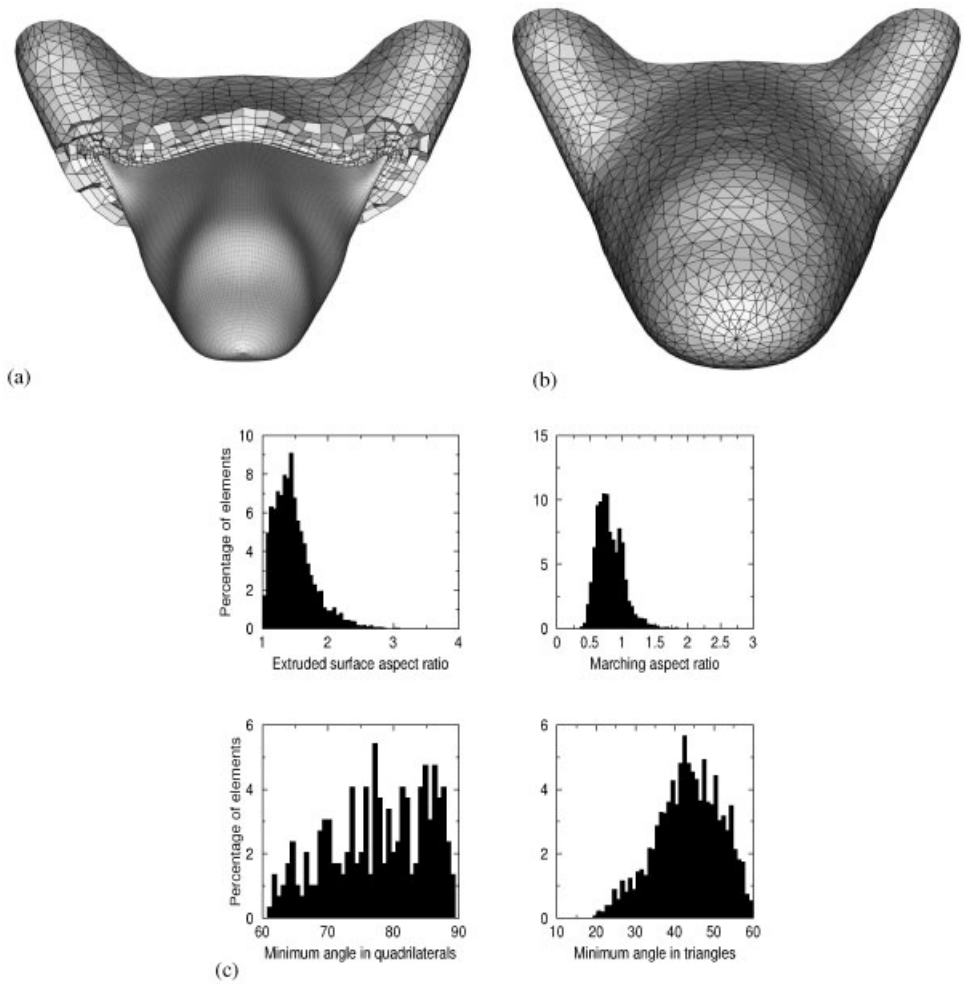

Figure 20. Notional x38 volume mesh generated by extruding seven layers with quality improvements: (a) cross section of the volume mesh; (b) outer surface mesh of the volume mesh; and (c) quality plots of the last layer of the volume mesh.

a cross section in the symmetry plane of the volume mesh generated by extruding 48 layers with quality improvements. Figures 23(a) and (b) show two different views of the outer surface of the volume mesh. It should be noted that it is not possible to generate a valid mesh with the same number of layers without quality improvements. The initial surface mesh has a few triangles with aspect ratios greater than 20 and angles less than 10°. Quality plots of the outer layer of the mesh are shown in Figure 24. These plots indicate a better extruded aspect ratio when compared with initial surface aspect ratio.

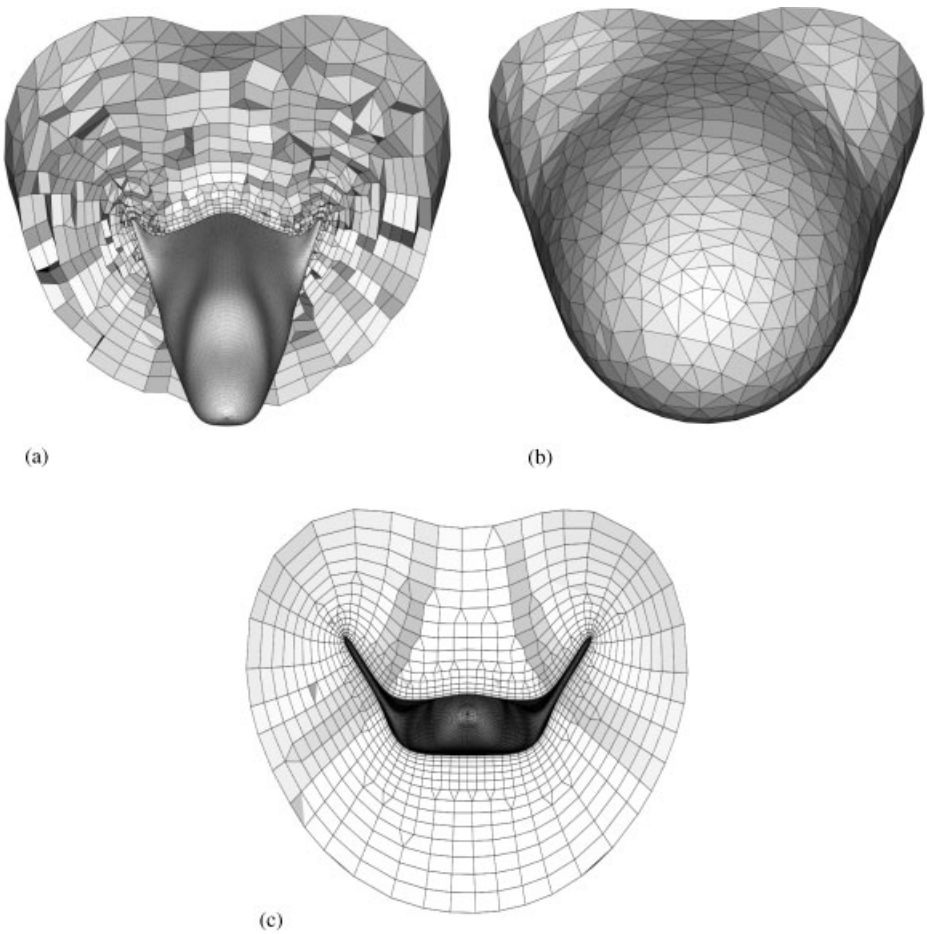

Figure 21. Notional x38 volume mesh generated by extruding 15 layers with quality improvements: (a) cross section of the extruded volume mesh; (b) outer surface of the volume mesh; and (c) rear view details of the volume mesh.

5. CONCLUSIONS

A method for generating extruded near-body volume meshes has been developed that exploits topologically adaptive generalized elements to improve local mesh quality. First, a two-layer reference mesh is generated from the layer initial surface mesh by extruding along the local surface normals. The reference mesh is then smoothed using a Poisson equation. As with any extruded mesh, quality may be degraded in concave and convex regions of the geometry as mesh lines coalesce or diverge, respectively. Quality improvement operations such as edge collapse, face refinement, and local reconnection are triggered by local geometric properties of the mesh and are performed in each layer to drive the mesh toward isotropy and improve the

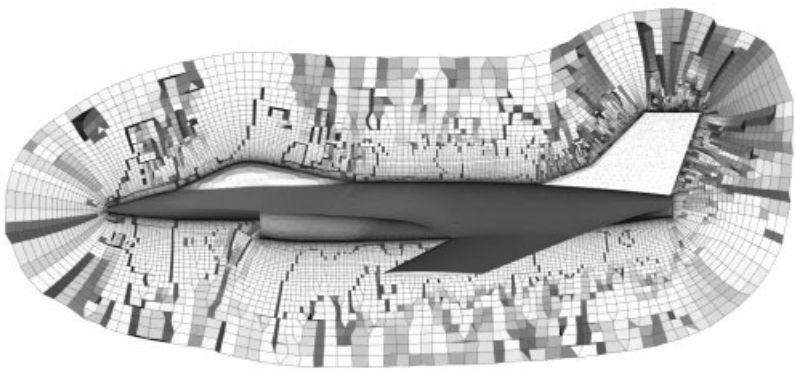

Figure 22. Cross section of the volume mesh for the fighter.

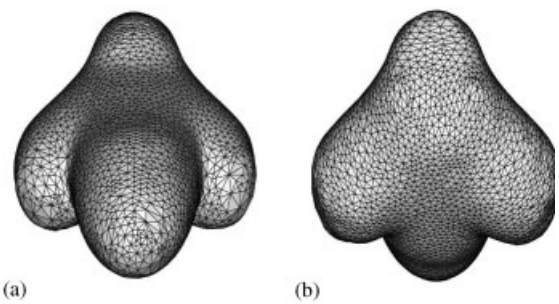

Figure 23. Outer surface mesh for the fighter: (a) outer surface of the volume mesh from front view; and (b) outer surface of the volume mesh from back view.

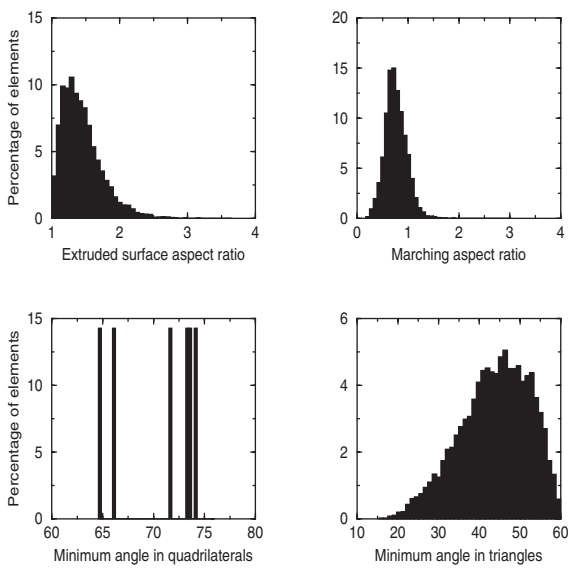

Figure 24. Quality plot of the last layer of the extruded volume mesh for the fighter.

transition from the extruded mesh to a void-filling tetrahedral mesh. A few examples along with mesh quality plots are presented to demonstrate the efficacy of this approach.

The results presented here demonstrate that the quality improvement process outlined in the paper significantly improves mesh quality as measured by face-based metrics. In so doing, the outer layer of the near-body extruded mesh provides a better surface upon which a void-filling tetrahedral mesh may be generated. These results illustrate the potential for the judicious use of general elements in an extruded mesh. One issue that remains to be addressed is that of an appropriate quality metric for general volume elements.

ACKNOWLEDGEMENTS

This effort was partially supported by NASA Glenn Research Centre (NAG2-2235), by NSF under the Information Technology Research Program (ACS-0085969), and by the Army Research Office (DAA 019-00-1-0155). The comments of the reviewers are also gratefully acknowledged.

REFERENCES

1. Chappell JA, Shaw JA, Leatham M. The generation of hybrids grids incorporating prismatic regions for viscous flow calculations. In *Numerical Grid Generation in Computational Field Simulations*, Cross M, Soni BK, Thompson JF, Hauser J, Eiseman PR (eds). NSF Engineering Research Center for Computational Field Simulations: Mississippi State, 1996; 537–546.
2. Pirzadeh S. Three-dimensional unstructured viscous grids by the advancing-layers method. *AIAA Journal* 1996; **34**(1):43–49.
3. Garimella VR, Shephard MS. Boundary layer meshing for viscous flows in complex domains. *Proceedings of the 7th International Meshing Roundtable 1998*, Sandia National Laboratories, 1998; 107–118.
4. Kallinderis Y. Hybrid grids and their applications. In *Handbook of Grid Generation*, Thompson JF, Soni BK, Weatherill NP (eds). CRC Press: Boca Raton, FL, 1998.
5. Thompson DS, Soni BK. Semistructured grid generation in three dimensions using a parabolic marching scheme. *AIAA Journal* 2002; **40**(2):391–393.
6. Leatham M, Stokes S, Shaw JA, Cooper J, Appa J, Blaylock TA. Automatic mesh generation for rapid-response Navier–Stokes calculations. *AIAA Paper* 2000-2247, 2000.
7. Cary A, Michal T. Generalized prisms for improved grid quality. *AIAA Paper* 2001-2552, Presented at 15th AIAA Computational Fluid Dynamics Conference, Anaheim, California, June 2001.
8. Koomullil RP, Soni BK. Generalized grid techniques in computational field simulation. In *Numerical Grid Generation in Computational Field Simulations*, Cross M, Eiseman PR, Hauser J, Soni BK, Thompson JF (eds). International Society for Grid Generation: Mississippi State, MS, 1998; 521–531.
9. Marcum DL. Generation of unstructured grids for viscous flow applications. *AIAA Paper* 1995-0212, Presented at AIAA 33rd Aerospace Sciences Meeting, Reno, NV, January 1995.
10. Tomaro RF, Strang WZ, Sankar LN. An implicit algorithm for solving time dependent flows on unstructured grids. *AIAA Paper* 1997-0333, Presented at AIAA 35th Aerospace Sciences Meeting, Reno, NV, January 1997.
11. Wu J, Tang L, Luke EA, Tong X-L, Cinnella P. Comprehensive numerical study of jet-flow impingement over flat plates. *Journal of Spacecraft and Rockets* 2002; **39**(3):337–366.
12. Thompson DS, Chalasani S, Soni BK. Generation of volume meshes by extrusion from surface meshes of arbitrary topology. *Proceedings of the 9th International Meshing Roundtable 2000*, Sandia National Laboratories, 2000; 385–393.
13. Noack RW. Solution-adaptive grid generation using parabolic differential equations. *AIAA Journal* 1990; **28**:1016–1023.
14. Knupp PM. Winslow smoothing on two-dimensional unstructured meshes. *Proceedings of the 7th International Meshing Roundtable 1998*, Sandia National Laboratories, 1998; 449–457.
15. Weatherill NP. Unstructured grids: procedures and applications. In *Handbook of Grid Generation*, Thompson JF, Soni BK, Weatherill NP (eds). CRC Press: Boca Raton, FL, 1998.

16. Wa K, Chen Z. A simple and effective mesh quality metric for hexahedral and wedge elements. *Proceedings of the 9th International Meshing Roundtable 2000*, Sandia National Laboratories, 2000; 325–333.
17. Owen S, Canann S, Saigal S. Pyramid elements for maintaining tetrahedra to hexahedra conformability. *Proceedings on Trends in Unstructured Mesh Generation*, AMD-vol. 220. 1997; 123–129.
18. Cobalt_{60} On-Line Documentation, Cobalt_{60}, September 1999, http://www.va.afrl.af.mil/vaa/vaac/COBALT/co_docs.html.
19. The Visualization Toolkit User's Guide, Kitware Inc.

